

# Investigation of Seismic Records of the 2011 off the Pacific Coast of Tohoku Earthquake at the Base of a Dam Site Using Two Source Models

Tsuneo OHSUMI<sup>1</sup>, Hiroshi ASAHLARA<sup>2</sup> and Masayuki KASHIWAYANAGI<sup>3</sup>

<sup>1</sup>Fellow Member of JSCE, Principal Research Fellow, Dr. Eng., Dr. Agr., Disaster Risk Research Unit,  
National Research Institute for Earth Science and Disaster Prevention (NIED)  
(3-1 Tennodai, Tsukuba, Ibaraki 303-0006, Japan)  
E-mail: t\_ohsumi@bosai.go.jp

<sup>2</sup>Member of JSCE, Senior Researcher, Dr. Eng., Research and Development,  
Advanced Simulation Technology of Mechanics, Co., Ltd.  
(Wako-Riken Incubation Plaza, 2-3-13, Minami, Wako, Saitama, 351-0104, Japan)  
E-mail: asahara@astom.co.jp

<sup>3</sup>Dr. Eng., Adviser, Research and development department, Chigasaki research institute,  
Electric Power Development Co., Ltd.  
(9-88, Chigasaki 1-Chome, Chigasaki, Kanagawa 253-0041, Japan)  
E-mail: masayuki\_kashiwayanagi@jpower.co.jp

Seismic waveforms of the 2011 off the Pacific coast of Tohoku Earthquake recorded at the base of a dam site in Fukushima prefecture were analyzed comparing bore-hole motion records of the KiK-net stations, and were reproduced on the empirical Green's function method. Three empirical Green's functions were prepared to five strong-motion-generation-areas (SMGAs) model, considering the spread of the fault area. The observed peak ground acceleration (PGA) values and Fourier spectra were roughly explained by the synthetic, but the observed PGA time could not be explained. So we synthesized using another fault model, SPGA model. The comparison of the observed and synthetic waves made it clear that nearly simultaneous arrivals of waves from SMGAs or SPGAs at off-shore Miyagi prefecture and off-shore Fukushima prefecture contributed the PGA value and the peak time at the target site.

**Key Words:** empirical Green's function method, the 2011 off the Pacific Coast of Tohoku Earthquake, strong-motion-generation-area (SMGA), strong-motion-pulse-generation-area (SPGA)

## 1. INTRODUCTION

Dam sites located in Tohoku area have recorded many seismic waveforms of the 2011 off the Pacific coast of Tohoku Earthquake, Japan, which occurred on March 11, 2011 (main shock,  $M_w$  9.0) and its aftershocks. Several kinds of rupture processes of the main shock have been proposed using teleseismic waveforms (e.g., Ide *et al.*, 2011<sup>1</sup>), Ammon *et al.*, 2011<sup>2</sup>) or strong motions (e.g., Furumura *et al.*, 2011<sup>3</sup>, Kurahashi and Irikura, 2011<sup>4</sup>). It is common that every rupture model shows complex rupture propagation though the results vary from the focused frequencies or the analysis methods. The authors reproduced the waveforms of the main shock using the empirical Green's function (EGF) method (Irikura, 1986<sup>5</sup>). The EGF method is a technique to synthesize seismic records of a large event using the recorded data at small events as Green's functions. After the second proposal of Japan Society of Civil Engineering (JSCE), following the Southern Hyogo

prefecture earthquake in 1995, simulation of earthquake ground motions using the Green's function approach for a potential rupturing fault, has been included in one of the seismic resistant design codes (JSCE, 1996). Since the EGF method mainly depends on and uses small ground motion histories, small events selected as Green's functions are necessary to share the same path and site effects with the target event. Seismic waveforms recorded at the base of dam sites are suitable for this analysis, where seismic motion is less affected by sedimentary layers. Seismic records at the base of dam sites are affected by the structure above at high frequency range. However, seismic records are not able to explain the peak time of the observation wave. Therefore this report calculates a pulse wave pattern seen at a few effects of the sedimentation layer of records, which located off-the-coast of Miyagi through off-the-coast of Ibaragi using the super asperities model (Nozu, 2012<sup>3</sup>). The agreement between the observed and calculated ground motions is quite satisfactory, es-

pecially for a frequency range of the waveforms (0.2-1.0 Hz) including near-source pulses.

## 2. WAVEFORM REPRODUCTION OF THE MAIN SHOCK

The target dam site is located in the Tohoku area, and the location is marked by a filled triangle in **Fig. 1**. This dam is a rock-fill dam. Seismographs are installed at the tops and the base of the dam. This site has recorded seismic waves of the main shock and its aftershocks. Seismic waveforms of horizontal upstream-downstream (orthogonal to the enclosing bund) component recorded at the base of the dam site were used in this study.

To simulate strong motions using EGF method, the characterized source model and the EGFs are needed. The characterized source model was constructed using Kurahashi and Irikura (2011)<sup>4)</sup> model, which consists of five strong-motion-generation-areas (SMGAs). EGFs were selected from the aftershock records and the past records prior to the main shock, considering the propagation path and the radiation characteristic from the source.

## 3. SELECTION OF THE EGF

The target dam site has nine seismic records other than that of the main shock, whose record length exceed 40 seconds and whose epicenters are inside or around the fault zone of the main shock. These nine records are the candidates for EGFs. The hypocenters and CMT solutions of these records are shown in **Fig. 1**. The source parameters of the main shock and the small events reported by the Japan Meteorological Agency (JMA) and the CMT solutions reported by F-net (Okada *et al.*, 2004<sup>7)</sup>) are shown in Table 1. Event-1 to -5 occurred after the main shock, whereas event-6 to -9 occurred prior to the main shock.

The small events' records used as EGFs have to share the propagation path and site effects as well as the radiation characteristic from the source. Event-8 (August 16, 2005,  $M_w$  7.1) was commonly selected as the EGF for SMGA 1 and 2. We call this event as EGF-A. In a similar way, event-6 (March 14, 2010,  $M_w$  6.5) was selected as the EGF for SMGA 3 and 4 (EGF-B), and event-7 (May 8, 2008,  $M_w$  6.8) was selected for SMGA 5 (EGF-C). Event-3 was not selected as an EGF, on the grounds that this event was not an inter-plate earthquake but an intra-slab one (Ohta *et al.*, 2011<sup>8)</sup>), although the epicenter was inside the fault zone. The moment magnitude of event-5 ( $M_w$  7.8) was too large to use as EGF.

The information of stress drop and fault area is needed to use the waveforms as EGF. The corner

frequencies of EGF-B and EGF-C were estimated using bore-hole motion records of KiK-net (Aoi *et al.*, 2000<sup>9)</sup>) as shown in **Fig. 2**. The stress drop of these small events was calculated from the corner frequency and seismic moment relation (Boore, 1983<sup>10)</sup>). The fault area of the small event was obtained by the circular crack model by Brune (1970<sup>11)</sup>, 1971<sup>12)</sup>). Conversely, the source models of EGF-A had been estimated (e.g., Kamae, 2006<sup>13)</sup>, Suzuki and Iwata, 2007<sup>14)</sup>). The estimated models showed that this earthquake consisted of two large slips. We decided the fault size of EGF-A considering total size of large slips. Stress drop was obtained from the size and seismic moment using the circular crack formula (Eshelby, 1957<sup>15)</sup>). In this study, the observed records used as the EGFs were band-pass-filtered from 0.15 Hz to 10 Hz, considering the reliable frequency range of the observed records.

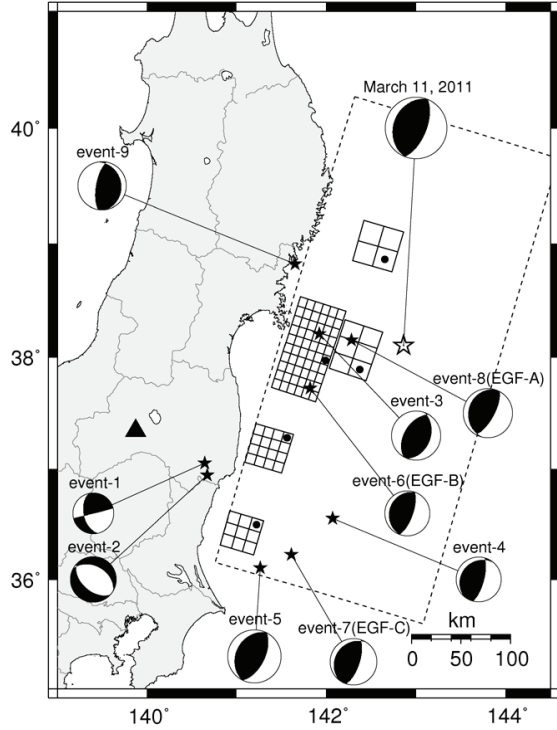


**Fig.1** The location of the target dam site (filled triangle), the fault zone (large dashed rectangle), characterized source model consisting of five SMGAs in the fault zone (small solid rectangles). The small rectangles and the closed circles inside them show the SMGAs and their initiation points. The open star and the closed stars show the epicenters of the main shock and the small events which are candidates for EGFs, respectively. EGF-A (for SMGA1, 2), B (for SMGA3, 4) and C (for SMGA5) are selected as EGFs. The target dam site is located in the Tohoku area, and the location is marked by a filled triangle.

#### 4. CHARACTERIZED SMGA SOURCE MODEL AND GROUND MOTION SIMULATION

The characterized source model was constructed using Kurahashi and Irikura (2011<sup>4)</sup>) model, slightly modifying the source parameters for our EGFs. The source parameters of each SMGA, such as the length, width, seismic moment, stress drop and delay time from the origin time of each SMGA are listed in **Table 1**. To calculate ground motions from each SMGA, the area of the SMGA was divided into equally-sized square sub faults, the area of which was set to be the same as the small events area as shown in **Fig. 1**. SMGA 1 and SMGA 3 are located off-shore Miyagi prefecture. SMGA 2, SMGA 4 and SMGA 5 are located off-shore Iwate prefecture, Fukushima prefecture and Ibaraki prefecture, respectively.

The rise times inside each SMGA were given by the empirical relations by Kataoka *et al.* (2003<sup>16)</sup>). The average S wave velocity and the rupture velocity were given to be 3.5 km/s and 2.8 km/s, respectively. The  $Q_s$  value for plate boundary earthquakes in Eastern Japan area, which was proposed by Kawase and Matsuo (2004<sup>17)</sup>), was used as the propagation property at this area;  $Q_s = 93 f^{0.89}$ ; Here  $f$  is frequency (Hz).

#### 5. DISCUSSION

Various segments of the Great Sumatra earthquakes (2004, 2013) were divided by their rupture speeds (Ishii *et al.*, 2005<sup>18)</sup>, Ya *et al.*, 2012<sup>19)</sup>). In this study, 3 empirical Green's functions are prepared by using 5 SMGAs models based on the records of the spread of the faults areas from small events.

Nearly simultaneous arrival from SMGAs at off-shore Miyagi and off-shore Fukushima contributed to the maximum acceleration value at the dam site (**Fig.3**).

**Table 1** The source parameters of the main shock and the small events which are candidates for EGFs. The origin times and the locations were determined by JMA. The CMT solutions and moments were reported by F-net. Stress drops and areas for EGFs were determined in this study.

	SMGA1	SMGA2	SMGA3	SMGA4	SMGA5
L (km)	55.2	36.8	92.0	36.8	34.5
W (km)	36.8	36.8	55.2	36.8	34.5
$N_x \times N_y \times L_D$	$3 \times 2 \times 7$	$2 \times 2 \times 3$	$10 \times 6 \times 11$	$4 \times 4 \times 4$	$3 \times 3 \times 2$
$M_0$ (Nm)	2.28E+21	6.52E+20	4.51E+21	4.37E+20	3.55E+20
Stress drop (MPa)	39.9	23.4	39.7	16.3	25.9
Delay time from origin time (sec)	15.64	66.42	68.41	109.71	118.17
Rise time (sec)	3.3	3.3	4.9	3.3	3.1
EGF	EGF-A	EGF-A	EGF-B	EGF-B	EGF-C

Although the main shock was  $M_w$  9.0, the epicenter

distance was about 300 kilometers; the maximum acceleration value was low level. The difference between the maximum acceleration 23 gal in this observation and 24 gal in this synthetic wave is not so significant. The maximum acceleration is reproducible although the seismic waves which were obtained from background regions other than SMGA areas are not considered in this simulation. Thus, it is thought that contribution from a background region is little effect. The preliminary tremor level at around 25 seconds of the observation waveform does not exist in a synthetic waveform. The preliminary tremor movements for 25 seconds are not recorded as small events. Large recorded levels only remain after the Share wave arrived. The synthetic waveform after dominant motion has two characteristic movements, which consists of the first half part of 20 seconds and the last half part of 70 seconds. It was able to reappear consisting of two dominant movements. The first half part of the synthetic waveform had a better reappearance than the observation waveform. The

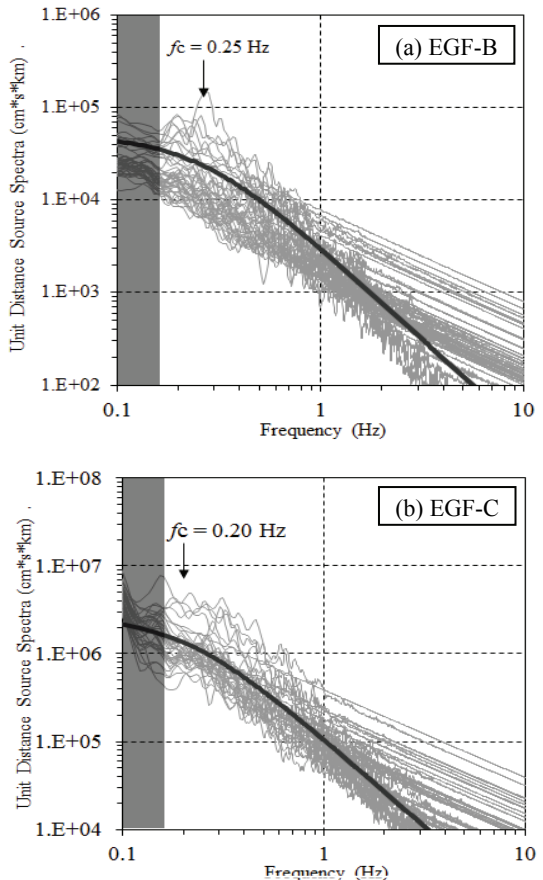


**Fig. 2** Displacement spectra estimated from bore-hole motion records at the KiK-net stations on rock from the small events ((a) EGF-B and (b) EGF-C) used as the empirical Green's functions. The shadow areas at low frequencies lower than 0.15 Hz show unreliable frequency range that was not used for the simulation.

waveform figures also differ.

The last half part of the synthetic waveform is a different, which is seen by observation during dominant movement. The observation waveform becomes larger at 75 seconds and 100 seconds. On the other hand, the synthetic waveform becomes larger at 85 seconds. In order to investigate this cause, the waveform is inspected from each areas of SMGA. According to **Fig.5**, the first 70 seconds is effected with only SMGA 1 area. The second strong motion is from the synthetic waveform at SMGA 3 and SMGA 4 areas. At SMGA 2 and SMGA 5 areas, the synthetic waveform is small, compared with other SMGA areas. In the observation waveform, an acceleration value of the dam axis direction becomes larger than the stream direction. The acceleration values exist at 25, 75 and 100 seconds.

Those wave arrival times correspond with the secondary wave arrival time from SMGA 1, SMGA 3, and SMGA 4 areas. According to **Fig.5**, the synthetic waveform in each SMGA area becomes gradually large after the secondary wave arrival time. It seems that a synthetic waveform has large amplitude at secondary wave arrival time. Although the epicenter model and the Green function are the causes, this paper does not describe this model.

The acceleration of the observation has a peak value at 100 seconds, which is addition of both SMGA3 and SMGA4 effects. The starting rupture time is delayed by 40 seconds (**Table 1**). However, the arrival time interval at the dam site is shortened by about 25 seconds (**Fig.4**). At SMGA 5 area, rupture propagation away from the dam site, the time difference of SMGA 4 and SMGA 5 areas becomes larger than the starting rupture time difference. This difference is based on the relative relationship of the SMGA area position and the dam site. And it is related to advance in the direction in which the rupture propagation moves in a fault area to the dam site. As a result, the addition to the effect of other SMGAs becomes small.

Comparison of the observation waveform and the synthetic waveform is in **Fig.3** with the Fourier spectrum. In the wide frequency domain, the spectrum of a synthetic waveform and the spectrum of the observation waveform are excellent. Composition of the observation and synthetic waveform is good at the peak frequencies of 0.36 Hz and 1.0 Hz. The Fourier spectrum shape appears in the depression at 1.8 Hz.

#### *Super asperities model*

In the source models of EGF, the peak record was not able to be synthesized at 156 seconds which did not appear in the envelope of an observation wave-

form. Although aimed at the wide range zone of 0.15~10 Hz for the source models of EGF, the super asperities model is synthesized by limiting to 0.2~1 Hz.

Nozu (2012)<sup>6)</sup> concentrated the simulation of the super asperities model at the frequency range of 0.2~1 Hz of the seismic records. In the observation point of a few effects of the sedimentary layers, which are located off-the-coast of Miyagi through to off-the-coast of Ibaraki using the super asperities model (**Table2**, **Fig.8**), pulse seismic waves have appeared clearly. This simulation of the ground motions is concentrated at a frequency range of the waveforms (0.2-1.0 Hz) including near-source pulses (**Fig.7**).

The KiK-net underground records the recorded waveforms, integrated as velocity waves and band pass filtered in the frequency range 0.2~1 Hz, are shown in **Fig.9**.

In the dam site record, the pulse with large amplitude has appeared at 156 seconds in each case. This pulse appeared also in the envelope waveforms (**Fig.5**); its first 3 peaks are not so clear in the velocity waveforms.

The first 3 peaks at frequency range higher than 1 Hz and the frequency range in lower than 1 Hz is not included. On the other hand, the acceleration peak had the frequency range of 0.2~1 Hz. In the synthetic waveform, the pulse appeared in 150 seconds. This peak did not appear in the next half in the synthetic waveform. The pulse, which appeared in the dam site records and also in the KiK-net observation records, is not a clear pulse as the observed waveform by Nozu and Wakai (2012).

Another characterized source model was constructed using Nozu and Wakai (2012)<sup>20)</sup>, which consists of nine strong-motion-pulse-generation-areas (SMGAs). An earthquake source parameter is shown in **Table 2**. The hypocenters and CMT solutions of these records are shown. The location of the target dam site, the fault zone, characterized source model consisting of nine SPGAs in the fault zone are shown in **Fig. 2**. Earthquake and strong ground motions are simulated based on site amplification and phase characteristics. Small events referred to Nozu and Wakai (2012). SPGA1, SPGA2 and SPGA3 chose Event-8 (EGF-A) of Table 1. SPGA9 was selected Event-7 (EGF-C) of Table 1. Other SPGA was selected a near the hypocenter. SPGA4 was selected as Event-8. SPGA5, SPGA6 and SPGA7 were selected as Event-6 (EGF-B).

Since the simulations were not estimating the Strong motion technique using site-specific amplification, it does not explain about the amplitude-spectrum of the synthetic waveforms.

The aim of simulations is reproduced velocity waveform and pulse time. Velocity waveform amplitude during the 150 seconds becomes larger than the 120 seconds before. The pulse at 156 seconds was increased by the stacking together of SPGA4, SPGA5, SPGA6 and SPGA7 pulse effects. In the

not as significant as the clear pulse such as Nozu (2012)<sup>6</sup> report. For the duration time of about 30 seconds, the observation point was far from SPGA. In addition, the earthquake motion of SPGA4 off Miyagi was an accumulation of SPGA5, SPGA6 and SPGA7 effects in the off Fukushima area.

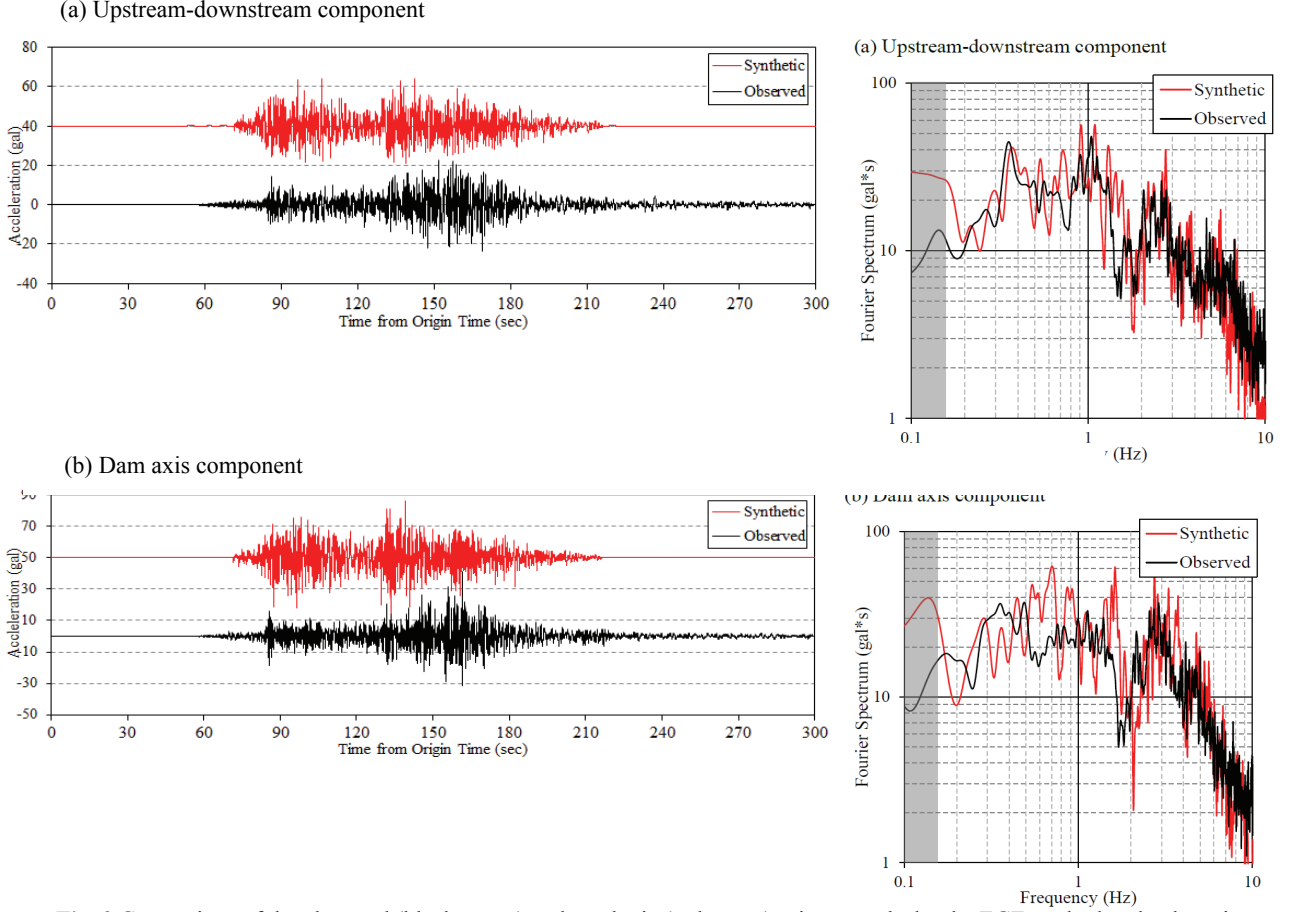


**Fig. 3** Comparison of the observed (black traces) and synthetic (red traces) seismographs by the EGF method at the dam site. The acceleration waveforms (left graph) and Fourier spectra (right graph) are composed. The waveforms performed filter processing to cut a low frequency than 0.15Hz.

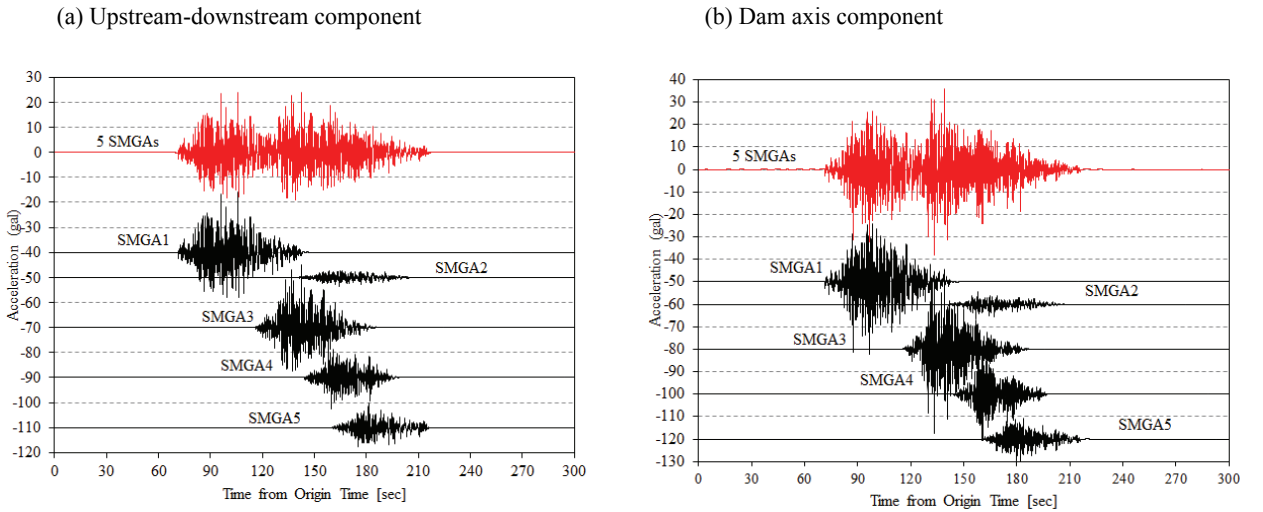


**Fig.4** Comparison of synthetic waveforms from five SMGAs (red trace) and from individual SMGAs (black traces) from SMGA1 to SMGA5. The waveforms performed filter processing to cut a low frequency than 0.15Hz. dam site or the nearby KiK-net observation sites was

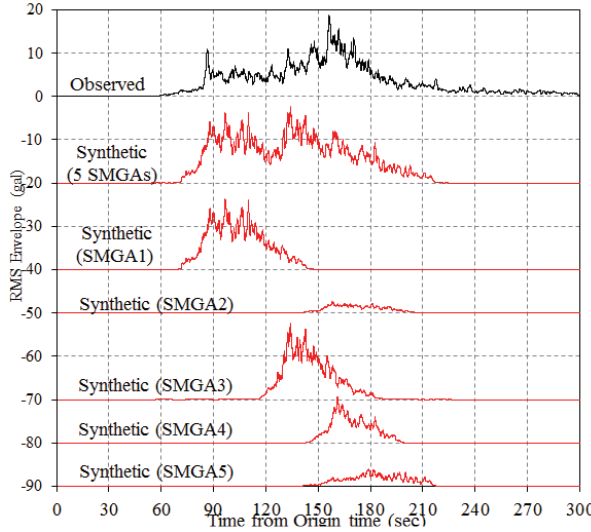


**Fig.5** Comparison of synthetic horizontal enveloped waveforms from five SMGAs (red trace) and from individual SMGAs (black traces) from SMGA1 to SMGA5. The waveforms performed filter processing to cut a low frequency than 0.15Hz.

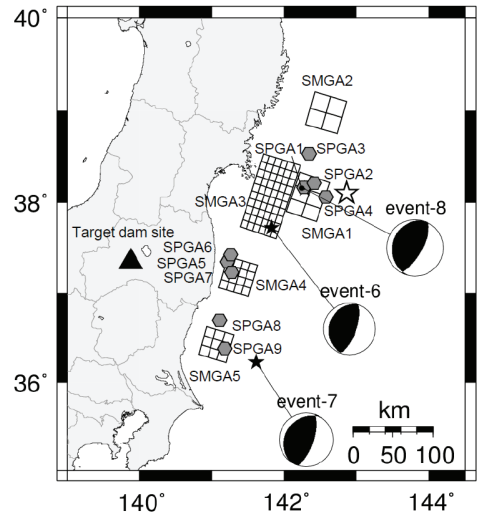


**Fig.7** The location of the target dam site (filled triangle), the fault zone (large dashed rectangle), characterized source model consisting of nine SPGAs in the fault zone (small solid rectangles).

**Table 2** The source parameters of each SPGA.

	SPGA1	SPGA2	SPGA3	SPGA4	SPGA5	SPGA6	SPGA7	SPGA8	SPGA9
$L$ (km)	3.0	4.0	4.0	3.5	3.0	3.0	6.0	8.0	7.0
$W$ (km)	2.0	3.0	2.0	3.0	4.0	4.0	2.0	3.0	7.0
$M$ (Nm)	8.00E+18	8.00E+18	4.00E+18	2.10E+19	3.00E+18	3.00E+18	5.00E+18	9.00E+18	2.00E+19
Slip (m)	28.3	14.1	10.6	42.4	5.3	5.3	8.8	8.0	8.7
Delay time from origin time (sec)	25.38	28.78	75.28	68.18	98.98	106.28	116.88	127.68	132.78
Rise time (sec)	0.17	0.25	0.17	0.25	0.33	0.17	0.25	0.17	0.25
EQ for Phase Effect	Event-8	Event-8	Event-8	Event-8	Event-6	Event-6	Event-6	Event-7	Event-7

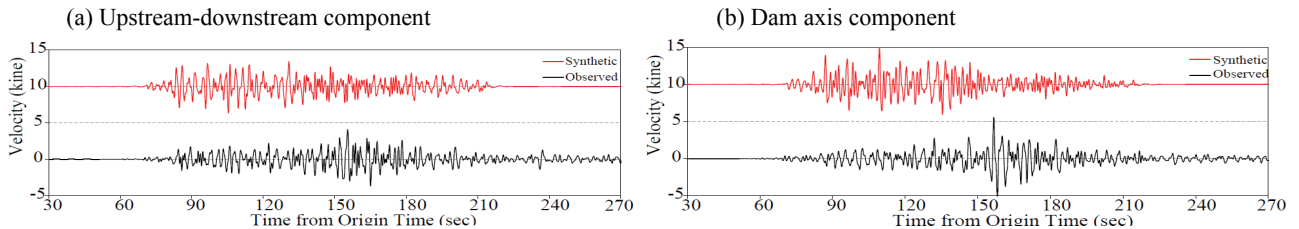


**Fig.6** Comparison of the observed (black traces) and synthetic (red traces) seismographs by the SPGA method at the dam site. The integrated velocity waveforms, which performed band pass filter processing from 0.2 to 1Hz.

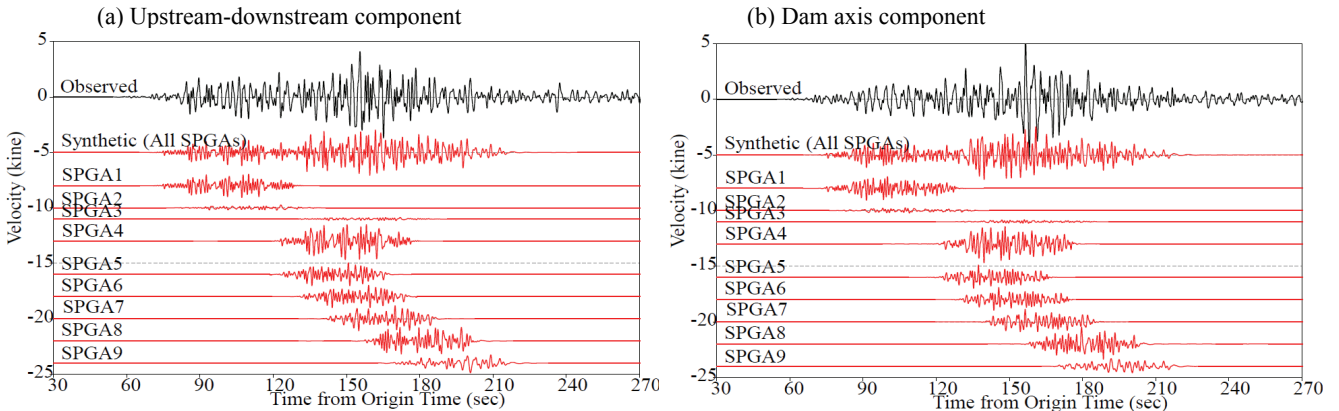


**Fig.8** Comparison of synthetic waveforms from nine SPGA s (red trace) and from individual SPGAs (black traces) from SPGA 1 to SPGA 9. The waveforms performed band pass filter processing from 0.2 to 1Hz.

## 6. CONCLUSION

The earthquake motion record obtained at the dam site located from the Tohoku district Pacific Ocean in Fukushima Prefecture in 2011 was reproduced using the experiential Green function method and the statistical Green function method.

The earthquake motion obtained by dam foundation has a subterranean earthquake motion feature similar to the KiK-net observation, and is not subject to most influences of the sedimentary layers near the surface.

When one side applied three Green functions to five SMGA(s) in the SMGA model of the size of several 10 km, about PGA and the Fourier spectrum, observations were able to be excellently obtained.

In comparison with the case where one Green function is applied to all the SMGA(s), the use of three Green functions the reproduced observations were much better.

Moreover, in comparison of the envelope, a SMGA which corresponds to the peak of an observation waveform existed. And it was understood how the earthquake motion from each SMGA formed the whole observation waveform.

As for the time when the acceleration in the second half of an observation waveform serves as the maximum, it turned out that the earthquake motions of SMGA3 off Miyagi and SMGA4 off Fukushima overlapped and increased.

In the SMGA model, since reappearance of the time when acceleration serves as the maximum, was not completed. The waveform composition was performed using the statistical Green function method by the SPGA model of one-side the size which is several kilometers. The amplitude of the second half became larger than the first half of the observation waveform.

The earthquake motions of SPGA4 off Miyagi, and SPGA5, 6 and 7 off Fukushima were over rapped and increased.

The relationship of SMGA-SPGA and the dam site records determined the maximum time of acceleration appearing in the SMGA model.

**ACKNOWLEDGMENT:** The authors are grateful to the National Institute for Earth Science and Disaster Prevention (NIED), Japan for providing strong motion data of the KiK-net and the CMT solutions by the F-net as Tokushia-university research group.

## REFERENCES

- 1) Ide, S., Baltay, A. and Beroza, G. C., 2011. "Shallow Dynamic Overshoot and Energetic Deep Rupture in the 2011 MW 9.0 Tohoku-Oki Earthquake." *Science*, **332**, No. 6036, 1426 – 1429.
- 2) Ammon, C. J., Lay, T., Kanamori, H. and Cleveland, M., 2011. "A rupture model of the 2011 off the Pacific coast of Tohoku Earthquake." *Earth Planets Space*, **63**, 693 – 696.
- 3) Furumura, T., Takemura, S., Noguchi, S., Takemoto, T., Maeda, T., Iwai, K. and Padhy, S., 2011. "Strong ground motions from the 2011 off-the Pacific-Coast-of-Tohoku, Japan (Mw = 9.0) earthquake obtained from a dense nationwide seismic network." *Landslides*, **8**, 333 – 338.
- 4) Kurahashi, S. and Irikura, K., 2011. "Source model for generating strong ground motions during the 2011 off the Pacific coast of Tohoku Earthquake." *Earth Planets Space*, **63**, 571 – 576.
- 5) Irikura, K., 1986. "Prediction of strong acceleration motion using empirical Green's function." *Proceeding of 7th Japan Earthquake Symposium*, 151 – 156, Japan Soceity of Civil Engineering (1996). "Proposal on earthquake resistance of civil engineering structures."
- 6) Nozu, A., 2011, A Super Asperity Model for the 2011 Off the Pacific Coast of Tohoku Earthquake, *J. JAEE*, **12**, 2, 21-40. (in Japanese with English abstract)
- 7) Okada, Y., Kasahara, K., Hori, S., Obara, K., Sekiguchi, S., Fujiwara, H. and Yamamoto, A., 2004. "Recent progress of seismic observation networks in Japan – Hi-net, F-net, K-NET and KiK-net–." *Earth Planets Space*, **56**, xv – xxviii.
- 8) Ohta, Y., Miura, S., Ohzono, M., Kita, S., Jinuma, T., Demachi, T., Tachibana, K., Nakayama, T., Hirahara, S., Suzuki, S., Sato, T., Uchida, N., Hasegawa, A. And Umino, N., 2011. "Large intraslab earthquake (2011 April 7 M7.1) after the 2011 off the Pacific coast of Tohoku earthquake (M9.0): Coseismic fault model based on the dense GPS network data." *Earth Planets Space*, **63**, 12, 1207-1211.
- 9) Aoi, S., Obara, K., Hori, S., Kasahara, K. and Okada, Y. , 2000. "New strong-motion observation network: KiK-net." *Eos Transactions AGU, Fall Meeting Suppl.*, Abstract S71A-05.
- 10) Boore, D.M., 1983. "Stochastic simulation of high-frequency ground motions based on seismological models of the radiated spectra." *Bulletin of the Seismological Society of America*, **73**, 6, 1865 – 1894.
- 11) Brune, J.N., 1970. "Tectonic stress and the spectra of seismic shear waves from earthquakes." *Journal of Geophysical Research*, **75**, 26, 4997 – 5009.
- 12) Brune, J.N., 1971. "Correction." *Journal of Geophysical Research*, **76**, 20, 5002.
- 13) Kamae, K., 2006. "Source modeling of the 2005 off-shore Miyagi prefecture, Japan, earthquake (MJMA=7.2) using the empirical Green's function method." *Earth Planets Space*, **58**, 1561 – 1566.
- 14) Suzuki, W. and Iwata, T., 2007. "Source model of the 2005 Miyagi-Oki, Japan, earthquake estimated from broadband strong motions." *Earth Planets Space*, **59**, 1155 – 1171.
- 15) Eshelby, J.D., 1957. "The determination of the elastic field of an ellipsoidal inclusion, and related problems." *Proceedings of the Royal Society A*, **241**, 1226, 376 – 396.
- 16) Kataoka, S., Kusakabe, T., Murakoshi, J. and Tamura, K., 2003. "Study on a Procedure for Formulating Level 2 Earthquake Motion Based on Scenario Earthquakes." *Research Report of National Institute for Land and Infrastructure Management*, 15. (in Japanese with English abstract)
- 17) Kawase, H. and Matsuo, H., 2004. "Separation of Source, Path and Site Effects based on the Observed Data by K-NET, KiK-net, and JMA Strong Motion Network." *Journal of JAEE*, **4**, 1, 33 – 52. (in Japanese with English abstract)

- abstract)
- 18) Ishii, M., Shearer, P. M., Houston, H. and Vidale, J. E.: Extent, duration and speed of the 2004 Sumatra-Andaman earthquake imaged by the Hi-Net array, *Nature*, **435**, 933 – 936, 2005.
  - 19) Yagi, Y., Nakao, A. & Kasahara, A., Smooth and rapid slip near the Japan Trench during the 2011 Tohoku-oki earthquake revealed by a hybrid back-projection method, *Earth Planet. Sci. Lett.*, 355–356, 15 November 2012, pp.94–101.
  - 20) Nozu, A., Wakai, J., 2012. A Source Model for the 2011 Off the Pacific Coast of Tohoku, Japan Earthquake to explain Strong Ground Motions, *Report of The Port and Airport Research Institute*, **51**, 1. (in Japanese with English abstract)

(Received ○○, 2013)